



# Synthetic and structural study on some new porphyrin or metalloporphyrin macrocycle-containing model complexes for the active site of [FeFe]-hydrogenases

Li-Cheng Song<sup>a,\*</sup>, Liang-Xing Wang<sup>a</sup>, Chang-Gong Li<sup>a</sup>, Fengyu Li<sup>b</sup>, Zhongfang Chen<sup>b,\*\*</sup>

<sup>a</sup> Department of Chemistry, State Key Laboratory of Elemento-Organic Chemistry, Nankai University, Tianjin 300071, China

<sup>b</sup> Department of Chemistry, Institute for Functional Nanomaterials, University of Puerto Rico, San Juan, PR 00931-3346, USA

## ARTICLE INFO

### Article history:

Received 12 June 2013

Received in revised form

27 August 2013

Accepted 5 September 2013

### Keywords:

Enzyme model

Hydrogenase

Iron

Metalloporphyrin

Porphyrin

Sulfur

## ABSTRACT

To mimic the natural enzymes [FeFe]-hydrogenases, some new porphyrin and metalloporphyrin moiety-containing model complexes, namely 5- $[p\text{-Fe}_2(\text{CO})_6(\mu\text{-SCH}_2)_2\text{CHO}_2\text{CC}_6\text{H}_4]$ , 10,15,20-triphenylporphyrin (**2**), 5- $[p\text{-Fe}_2(\text{CO})_6(\mu\text{-SCH}_2)_2\text{CHO}_2\text{CC}_6\text{H}_4]$ , 10,15,20-triphenylporphyrinozinc (**3**), 5- $[p\text{-Fe}_2(\text{CO})_6(\mu\text{-SCH}_2)_2\text{NC}_2\text{H}_4\text{SC}_6\text{H}_4]$ , 10,15,20-triphenylporphyrin (**7**), and 5- $[p\text{-Fe}_2(\text{CO})_5(\mu\text{-SCH}_2)_2\text{NC}_2\text{H}_4\text{SC}_6\text{H}_4]$ , 10,15,20-triphenylporphyrin (**8**), have been successfully prepared by our designed synthetic routes involving the corresponding precursor compounds  $[(\mu\text{-SCH}_2)_2\text{CHO}_2\text{CC}_6\text{H}_4\text{CHO-}p]\text{Fe}_2(\text{CO})_6$  (**1**),  $p\text{-Boc-NHC}_2\text{H}_4\text{SC}_6\text{H}_4\text{CHO}$  (**4**), 5- $(p\text{-Boc-NHC}_2\text{H}_4\text{SC}_6\text{H}_4)$ , 10,15,20-triphenylporphyrin (**5**), and 5- $(p\text{-NH}_2\text{C}_2\text{H}_4\text{SC}_6\text{H}_4)$ , 10,15,20-triphenylporphyrin (**6**). All these new compounds **1–8** have been characterized by elemental analysis and various spectroscopic methods, and particularly for **1–3** and **7** by X-ray crystallography. In addition, the density functional theory computations on **8** were performed to assist its structural characterization.

© 2013 Elsevier B.V. All rights reserved.

## 1. Introduction

Hydrogenases are natural enzymes that catalyze the reversible redox reaction between proton and hydrogen in various microorganisms [1]. According to the metal content in the active site, hydrogenases are primarily classified as [FeFe]-hydrogenases ([FeFe]Hases), [NiFe]-hydrogenases ([NiFe]Hases), and [Fe]-hydrogenases (Hmd) [2–8]. While [FeFe]Hases are mainly used for proton reduction to hydrogen, [NiFe]Hases are employed for hydrogen oxidation to protons [9–11], Hmd is utilized to activate hydrogen for use in catabolic processes of microorganisms [7,8]. Currently, [FeFe]Hases are receiving more attention over [NiFe]Hases and Hmd, because of their unusual structures and particularly their extremely rapid rates for production of “clean” and highly efficient H<sub>2</sub> fuel [12,13]. Recent X-ray crystallography [14–16] and FTIR spectroscopy [17–19] revealed that the active site of [FeFe]Hases, so-called H-cluster [9], consists of a cubane-like [Fe<sub>4</sub>S<sub>4</sub>] cluster that

is linked to a butterfly [Fe<sub>2</sub>S<sub>2</sub>] cluster via the cysteinyl S atom. In addition, the two iron atoms of the [Fe<sub>2</sub>S<sub>2</sub>] cluster are bridged by a propanedithiolate (PDT), azadithiolate (ADT), or oxadithiolate (ODT) ligand and are coordinated by a given amount of CO and CN<sup>−</sup> ligands (Fig. 1).

Encouraged by the structural studies on H-cluster, the synthetic chemists have designed and synthesized a variety of structural and functional models for the active site of [FeFe]Hases [20–38]. Among these models, the porphyrin or metalloporphyrin-containing models are of particular interest, since they belong to the dyads light-driven type models in which the photosensitizer porphyrin or metalloporphyrin is covalently or coordinatively attached to a simple diiron model complex. To date, although several such model complexes have been prepared [34–38], none of them contains the photosensitizer porphyrinylester or metalloporphyrinylester moiety that is covalently attached to a simple diiron model (such as **2** and **3** in Fig. 2) or includes a porphyrinylthioether moiety that is covalently or coordinatively bound to a simple diiron model (such as **7** and **8** in Fig. 2). To develop the synthetic methodology for such new types of porphyrin or metalloporphyrin-containing H-cluster model complexes, we initiated this study. Herein we report the results of this study.

\* Corresponding author.

\*\* Corresponding author.

E-mail addresses: [lcsong@nankai.edu.cn](mailto:lcsong@nankai.edu.cn) (L.-C. Song), [zhongfangchen@gmail.com](mailto:zhongfangchen@gmail.com) (Z. Chen).

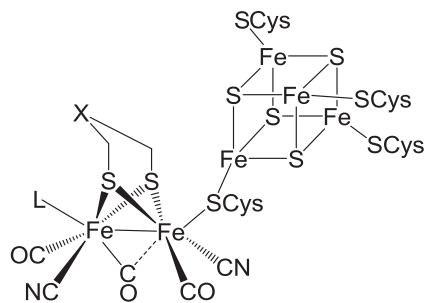


**Fig. 1.** The simplified structure of H-cluster in different functional states (L = H<sub>2</sub>O, CO, H, or H<sub>2</sub>; X = CH<sub>2</sub>, NH, or O).

## 2. Results and discussion

**2.1. Synthesis and spectroscopic characterization of simple model complex [( $\mu$ -SCH<sub>2</sub>)<sub>2</sub>CHO<sub>2</sub>CC<sub>6</sub>H<sub>4</sub>CHO-*p*][Fe<sub>2</sub>(CO)<sub>6</sub>] (**1**) and the porphyrin or metalloporphyrin-containing model complexes 5-[*p*-Fe<sub>2</sub>(CO)<sub>6</sub>( $\mu$ -SCH<sub>2</sub>)<sub>2</sub>CHO<sub>2</sub>CC<sub>6</sub>H<sub>4</sub>], 10,15,20-triphenylporphyrin (**2**) and 5-[*p*-Fe<sub>2</sub>(CO)<sub>6</sub>( $\mu$ -SCH<sub>2</sub>)<sub>2</sub>CHO<sub>2</sub>CC<sub>6</sub>H<sub>4</sub>], 10,15,20-triphenylporphyrin zinc (**3**)**

According to our designed synthetic route for preparation of the porphyrinylester or metalloporphyrinylester moiety-containing model complexes **2** and **3**, we should first prepare the simple *p*-formylbenzoate functionalized model complex **1**. The treatment of the C-hydroxy functionalized complex [( $\mu$ -SCH<sub>2</sub>)<sub>2</sub>CH(OH)]Fe<sub>2</sub>(CO)<sub>6</sub> with *p*-formylbenzoyl chloride (prepared in situ by reaction of *p*-formylbenzoic acid with SOCl<sub>2</sub>) [39] in CH<sub>2</sub>Cl<sub>2</sub> in the presence of Et<sub>3</sub>N gave the simple model complex **1** in 62% yield. Further treatment of **1** with benzaldehyde and pyrrole in 1:3:4 M ratio in the presence of BF<sub>3</sub>·OEt<sub>2</sub>, followed by treatment with oxidant *p*-chloranil afforded model complex **2** in 21% yield along with tetraphenylporphyrin (TPP) in 18% yield. Finally, the metalloporphyrinylester moiety-containing model complex **3** was produced by reaction of **2** in CHCl<sub>3</sub> with Zn(OAc)<sub>2</sub> in MeOH at room temperature in 88% yield (Scheme 1).

Complexes **1–3** are air-stable red solids, which have been characterized by elemental analysis and spectroscopy. For instance, the IR spectra of **1–3** displayed three to four absorption bands in the region 2075–1992 cm<sup>-1</sup> for their terminal carbonyls

and one absorption band in the range 1706–1722 cm<sup>-1</sup> for their organic carbonyls, respectively. In addition, **2** and **3** showed three absorption bands in the region 1558–1339 cm<sup>-1</sup> assigned to the skeleton vibrations of pyrrole rings in their porphyrin and porphyrin zinc macrocycles, respectively [40]. The <sup>1</sup>H NMR spectra of **1–3** showed a broad singlet or a multiplet at about 4.6 ppm for their bridgehead C-attached axial hydrogen atoms, whereas **2** exhibited a singlet at -2.80 ppm for the two protons attached to N atoms in its pyrrole rings [41]. The UV–vis spectra of **2** and **3** were determined in CH<sub>2</sub>Cl<sub>2</sub>, which showed one Soret band at 412 and 414 nm in the near-UV region, respectively. In addition, **2** displayed four Q bands in the range 514–645 nm, whereas **3** exhibited two Q bands at 548 and 586 nm in the visible region. Apparently, the different Q bands displayed by **2** and **3** are caused by the different photosensitizer moieties [34,35], namely the porphyrinylester moiety for **2** and the metalloporphyrinylester moiety for **3**.

## 2.2. Crystal structures of **1–3**

The molecular structures of **1–3** were unambiguously confirmed by X-ray diffraction techniques (Fig. 3–5, Table 1–3). As can be seen intuitively from Fig. 3, complex **1** contains a diiron PDT moiety in which the six-membered ring Fe1S1C7C8C9S2 has a chair conformation and the other six-membered ring Fe2S1C7C8C9S2 a boat conformation. The *p*-formylbenzoate group is attached to the common C8 atom of the two six-membered rings by an equatorial bond and a hydrogen atom is attached to C8 by an axial bond. Both Fe1 and Fe2 atoms adopt the expected square-pyramidal geometry and the Fe1–Fe2 bond length (2.5007 Å) is very close to the corresponding those of its parent complex [( $\mu$ -SCH<sub>2</sub>)<sub>2</sub>CH(OH)]Fe<sub>2</sub>(CO)<sub>6</sub> and similar diiron complexes [26,42–44].

Fig. 4 shows that complex **2** has the same diiron PDT moiety as **1**, but the equatorial *p*-formylbenzoate group in **1** has been replaced by an equatorial porphyrinylester moiety. In the porphyrin cycle the C–N bond lengths in pyrrole rings are nearly the same (1.366–1.380 Å), which lie between those of normal single and double C–N bonds [45]. It is worth pointing out that the four benzene rings attached to porphyrin cycle is planar and twisted relative to the porphyrin plane in order to reduce the steric interactions between the phenyl hydrogen atoms proximal to the porphyrin cycle and the pyrrole rings.

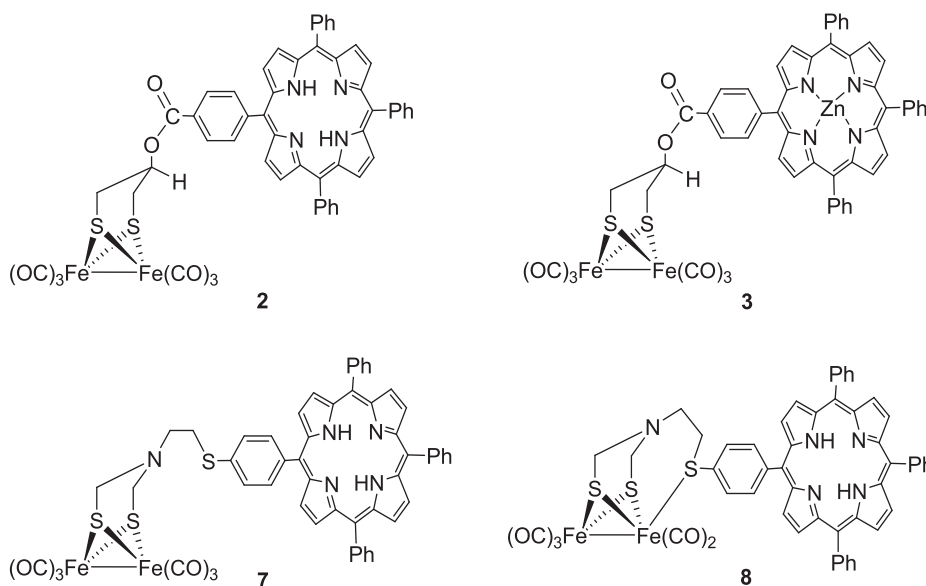
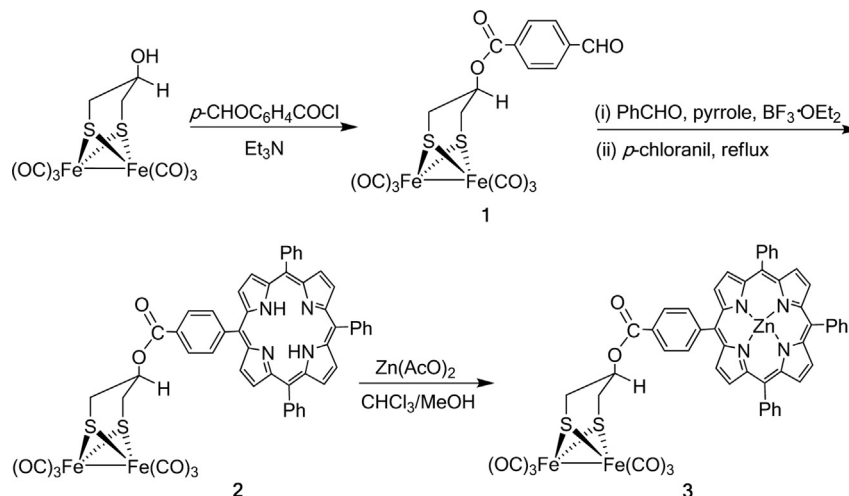


**Fig. 2.** The target light-driven models **2**, **3**, **7**, and **8** reported in this article.



Scheme 1. Synthetic routes of 1–3.

As can be seen in Fig. 5, the structure of **3** is almost identical with that of **2**, except the parent porphyrin macrocycle is replaced by a porphyrinozinc macrocycle. It is noteworthy that in the structure of **3** there is one molecule of MeOH axially coordinated to Zn1 atom with a Zn–O9 bond length of 2.116 Å. The coordinated MeOH was obviously originated from the mixed solvent *o*- $\text{Cl}_2\text{C}_6\text{H}_4/\text{MeOH}$  used in the single-crystal growing process. The Fe1–Fe2 bond length (2.5077 Å) is very close to the corresponding those of its parent complex and similar diiron complexes [26,42–44]. The four benzene rings around the metalloporphyrin moiety are also twisted relative to the porphyrin plane with a dihedral angle from 66.8° to 87.2° in order to reduce the steric repulsions between the proximal hydrogen atoms of the benzene and pyrrole rings in the metalloporphyrin macrocycle.

**2.3. Synthesis and spectroscopic characterization of precursor compounds *p*-Boc-NHC<sub>2</sub>H<sub>4</sub>SC<sub>6</sub>H<sub>4</sub>CHO (**4**), 5-(*p*-Boc-NHC<sub>2</sub>H<sub>4</sub>SC<sub>6</sub>H<sub>4</sub>), 10,15,20-triphenylporphyrin (**5**), 5-(*p*-NH<sub>2</sub>C<sub>2</sub>H<sub>4</sub>SC<sub>6</sub>H<sub>4</sub>), 10,15,20-triphenylporphyrin (**6**), and the porphyrin-containing model complexes 5-[*p*-Fe<sub>2</sub>(CO)<sub>6</sub>(μ-SCH<sub>2</sub>)<sub>2</sub>NC<sub>2</sub>H<sub>4</sub>SC<sub>6</sub>H<sub>4</sub>], 10,15,20-triphenylporphyrin (**7**) and 5-[*p*-Fe<sub>2</sub>(CO)<sub>5</sub>(μ-SCH<sub>2</sub>)<sub>2</sub>NC<sub>2</sub>H<sub>4</sub>SC<sub>6</sub>H<sub>4</sub>], 10,15,20-triphenylporphyrin (**8**)**

In order to prepare the designed two porphyrinylthioether-containing model complexes **7** and **8**, we first prepared their precursor compounds **4–6**. The treatment of Boc-NHC<sub>2</sub>H<sub>4</sub>SH (Boc = *tert*-butoxycarbonyl) with KOH in EtOH and subsequent treatment of the resulting potassium mercaptide Boc-NHC<sub>2</sub>H<sub>4</sub>SK with *p*-ClC<sub>6</sub>H<sub>4</sub>CHO resulted in formation of precursor **4** in 50% yield. Further treatment of **4** with benzaldehyde, pyrrole, and  $\text{BF}_3 \cdot \text{OEt}_2$  in  $\text{CH}_2\text{Cl}_2$  at room temperature, followed by treatment of the resulting mixture with the oxidant *p*-chloranil afforded TPP and precursor **5**

in 25% and 20% yields, respectively. Precursor **6** was obtained in 86% yield by removal of the Boc group from **5**, which was realized by treating **5** with a HCl (2 mol L<sup>-1</sup>) solution in 1:1 (v/v) THF and AcOEt (Scheme 2).

With the availability of precursors **4–6**, we started to prepare the target model complexes **7** and **8** by a sequential reaction involving (i) reaction of (μ-S<sub>2</sub>)Fe<sub>2</sub>(CO)<sub>6</sub> with LiBET<sub>3</sub>H in THF at –78 °C followed by treating (μ-LiS)<sub>2</sub>Fe<sub>2</sub>(CO)<sub>6</sub> with CF<sub>3</sub>CO<sub>2</sub>H to give (μ-HS)<sub>2</sub>Fe<sub>2</sub>(CO)<sub>6</sub> [46]; (ii) in situ reaction of (μ-HS)<sub>2</sub>Fe<sub>2</sub>(CO)<sub>6</sub> with 40% aqueous formaldehyde in THF from –78 °C to room temperature to yield (μ-HOCH<sub>2</sub>S)<sub>2</sub>Fe<sub>2</sub>(CO)<sub>6</sub> [47]; (iii) in situ reaction of (μ-HOCH<sub>2</sub>S)<sub>2</sub>Fe<sub>2</sub>(CO)<sub>6</sub> with **6** to afford model **7** in 51% yield; and (iv) final reaction of the isolated **7** with decarbonylating agent Me<sub>3</sub>NO·2H<sub>2</sub>O in  $\text{CH}_2\text{Cl}_2/\text{MeCN}$  at room temperature to produce model **8** in 88% yield (Scheme 3).

Precursors **4–6** are all air-stable solids, which have been characterized by elemental analysis and spectroscopic techniques. For example, the IR spectrum of **4** showed two absorption bands at 1682 and 1691 cm<sup>-1</sup> for its aldehyde and ester carbonyl groups, whereas **5** and **6** exhibited three absorption bands in the range of 1558–1349 cm<sup>-1</sup> for the skeleton vibrations of the pyrrole rings in their porphyrin moieties [40]. The <sup>1</sup>H NMR spectrum of **4** displayed a singlet at 9.93 ppm for its benzaldehyde CHO group, whereas **5** and **6** exhibited a singlet at –2.78 and –2.77 ppm for the NH groups in their porphyrin moieties [41]. In addition, the <sup>1</sup>H NMR spectra of **4** and **5** displayed a singlet at 4.90 and 5.09 ppm for the NH groups attached to their ester carbonyls, whereas **6** showed a singlet at 2.50 ppm for its NH<sub>2</sub> group.

Complexes **7** and **8** are also air-stable solids, which have been characterized by elemental analysis and spectroscopy. The IR spectra of **7** and **8** showed three to five absorption bands in the

**Table 1**  
Selected bond lengths (Å) and angles (°) for **1**.

Bond lengths			
Fe(1)–S(2)	2.2555(7)	Fe(1)–S(1)	2.2430(7)
Fe(1)–C(1)	1.806(3)	Fe(1)–Fe(2)	2.5007(5)
Fe(2)–S(2)	2.2490(7)	Fe(2)–S(1)	2.2618(7)
O(8)–C(10)	1.999(3)	O(9)–C(17)	1.201(3)
Bond angles			
Fe(2)–Fe(1)–S(1)	56.640(18)	Fe(2)–Fe(1)–S(2)	56.153(19)
Fe(1)–Fe(2)–S(2)	56.403(18)	Fe(1)–Fe(2)–S(1)	55.922(19)
S(1)–Fe(2)–S(2)	84.68(2)	Fe(1)–S(2)–Fe(2)	67.444(19)
Fe(2)–S(1)–Fe(1)	67.439(19)	C(7)–C(8)–O(7)	106.88(17)

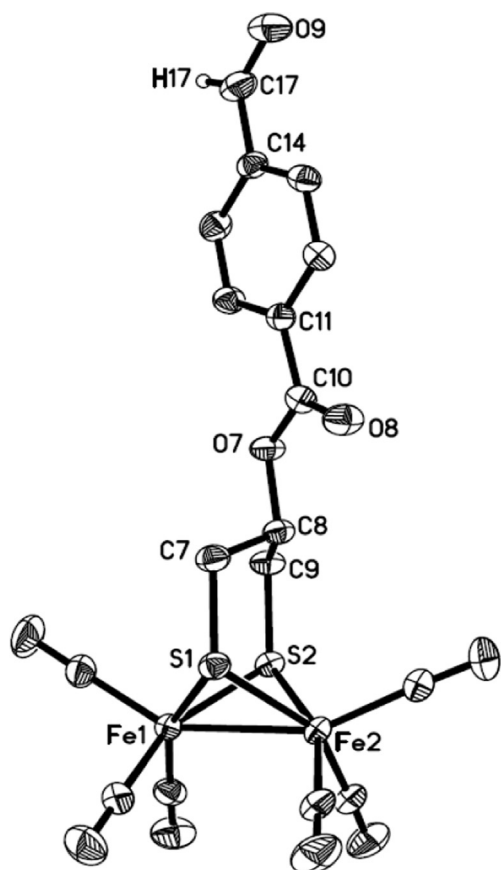
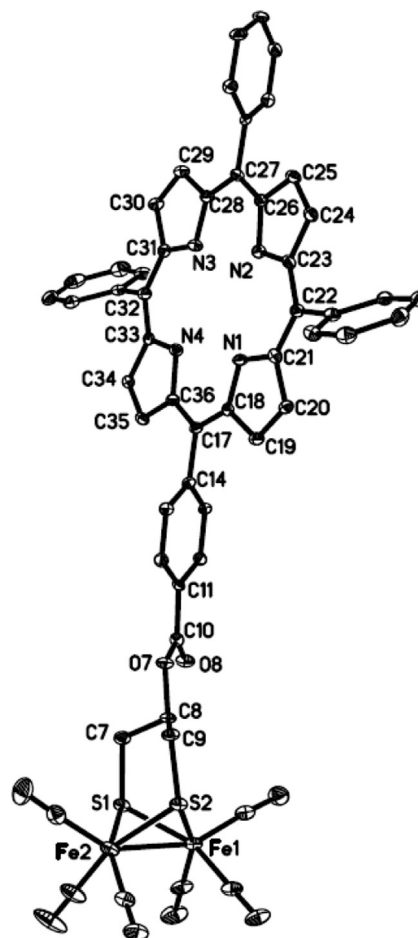
**Table 2**  
Selected bond lengths (Å) and angles (°) for **2**.

Bond lengths			
Fe(1)–S(1)	2.2680(15)	Fe(2)–S(2)	2.2560(14)
Fe(1)–S(2)	2.2701(14)	C(8)–O(7)	1.467(5)
Fe(2)–S(1)	2.2491(15)	Fe(1)–Fe(2)	2.5071(11)
N(1)–C(18)	1.380(6)	C(14)–C(17)	1.508(6)
Bond angles			
S(1)–Fe(1)–S(2)	84.62(5)	C(21)–N(1)–C(18)	109.6(4)
S(1)–Fe(1)–Fe(2)	55.93(4)	C(23)–N(2)–C(26)	106.6(4)
S(1)–Fe(2)–S(2)	85.39(5)	S(2)–Fe(1)–Fe(2)	56.10(4)
Fe(2)–S(2)–Fe(1)	67.27(4)	Fe(2)–S(1)–Fe(1)	67.42(5)

**Table 3**  
Selected bond lengths (Å) and angles (°) for **3**.

Bond lengths			
Fe(1)–S(1)	2.252(3)	Zn(1)–N(1)	2.061(6)
Fe(1)–S(2)	2.244(2)	Fe(1)–Fe(2)	2.5077(17)
Fe(2)–S(2)	2.246(2)	C(46)–O(2)	1.474(8)
Fe(2)–S(1)	2.273(2)	N(1)–C(41)	1.390(8)
Bond angles			
N(2)–Zn(1)–N(1)	88.8(2)	S(1)–Fe(1)–S(2)	85.68(9)
S(1)–Fe(1)–Fe(2)	56.74(7)	S(1)–Fe(2)–S(2)	85.13(9)
O(2)–C(46)–C(47)	106.6(5)	S(1)–Fe(2)–Fe(1)	55.94(7)
N(1)–Zn(1)–N(3)	164.1(2)	C(41)–N(1)–C(44)	107.4(6)

range of 2070–1935  $\text{cm}^{-1}$  assigned to their terminal carbonyls, and three absorption bands in the region 1558–1348  $\text{cm}^{-1}$  attributed to the skeletal vibrations of the pyrrole rings in their porphyrin moieties [40]. In addition, the  $^1\text{H}$  NMR spectrum of **7** displayed two triplets at 3.10 and 3.23 ppm for the two  $\text{CH}_2$  groups between the bridgehead N atom and the S atom attached to porphyrin moiety, whereas **8** exhibited two doublets at 3.29 and 3.69 ppm for the corresponding two  $\text{CH}_2$  groups, respectively. Note that the  $^1\text{H}$  NMR signals for the two  $\text{CH}_2$  groups of **8** is shifted downfield by ca. 0.2–0.5 ppm compared to those corresponding to **7**. This is obviously because the S atom in **8** is coordinated to Fe atom and in turn to cause the decrease of the electron density around the two  $\text{CH}_2$  groups. In addition, the  $^1\text{H}$  NMR spectra of **7** and **8** displayed a singlet at ca. –2.7 ppm for the NH groups in their porphyrin macrocycle [41]. The UV–vis spectra of **7** and **8** determined in  $\text{CH}_2\text{Cl}_2$  all showed one Soret band at 418 nm in the near-UV region. In addition, **7** and **8** displayed almost identical four Q bands at 515, 550, 591, and

**Fig. 3.** ORTEP view of **1** with 30% probability level ellipsoids.**Fig. 4.** ORTEP view of **2** with 30% probability level ellipsoids.

645 nm for **7** and at 514, 550, 591, and 645 nm for **8** in the visible region. This is because they contain the same photosensitizer porphyrinylthioether moiety and the coordination mode of this photosensitizer, either covalently or coordinatively, has no actual influence upon their UV–vis spectra.

#### 2.4. Crystal structure of **7** and DFT computations on **8**

The molecular structure of model complex **7** was unequivocally confirmed by X-ray diffraction analysis. While the ORTEP view of model complex **7** is presented in Fig. 6, Table 4 lists its selected bond lengths and angles.

Similar to the previously reported porphyrin-containing ADT-type model complexes [34–36], complex **7** was unequivocally confirmed to contain a diiron–ADT unit in which a boat-shaped six-membered ring N1C7S2Fe1S1C8 is fused to a chair-shaped six-membered ring N1C7S2Fe2S1C8. The diiron–ADT unit is connected via its bridgehead N1 atom to C11 atom of the porphyrin moiety (Note that N1–C9 is the common axial bond of the two fused six-membered rings). In the porphyrin moiety, the four benzene rings are twisted relative to the porphyrin plane with a dihedral angle from 56.3 to 83.2° in order to reduce the strong steric repulsions between the phenyl hydrogen atoms proximal to porphyrin moiety and the pyrrole rings. In addition, the porphyrin plane is nearly perpendicular to the S1S2C7C8 plane with a dihedral angle of 84.6°. While the C–N bond lengths in pyrrole rings of the porphyrin moiety are almost the same (1.366–1.379 Å) and are between those of normal single and double C–N bonds [45], the

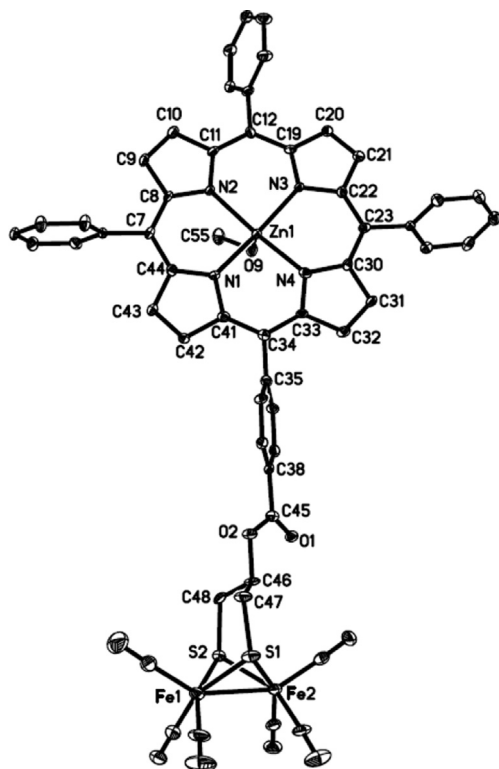


Fig. 5. ORTEP view of **3** with 30% probability level ellipsoids.

Fe1–Fe2 bond length (2.511 Å) is slightly shorter than the corresponding bond length in the reduced state of the natural enzyme (2.55 Å) [16].

Since the crystal structure of model complex **8** was not obtained due to lack of the qualified single-crystal for X-ray diffraction analysis, we performed the density functional theory (DFT) computations to assist its structural characterization. Fig. 7 shows the DFT optimized molecular structure of **8**, whereas some of the calculated bond lengths and angles are given in Table 5. As can be seen in Table 5, the calculated bond lengths and angles of **8** are very close to the corresponding those of **7** determined by X-ray diffraction analysis. In addition, the calculated Fe1–S3 bond length (2.275 Å) of **8** (namely the distance between its thioether S atom and one Fe atom in its diiron subsite) is very close to the corresponding Fe–S bond lengths of the previously reported simple model complexes, such as  $[(\mu\text{-SCH}_2)_2\text{NCH}_2\text{CH}_2\text{SMe}]\text{Fe}_2(\text{CO})_5$  (2.270 Å) [26],  $[(\mu\text{-SCH}_2)_2\text{C}(\text{Me})\text{CH}_2\text{SMe}]\text{Fe}_2(\text{CO})_5$  (2.254 Å) [48]

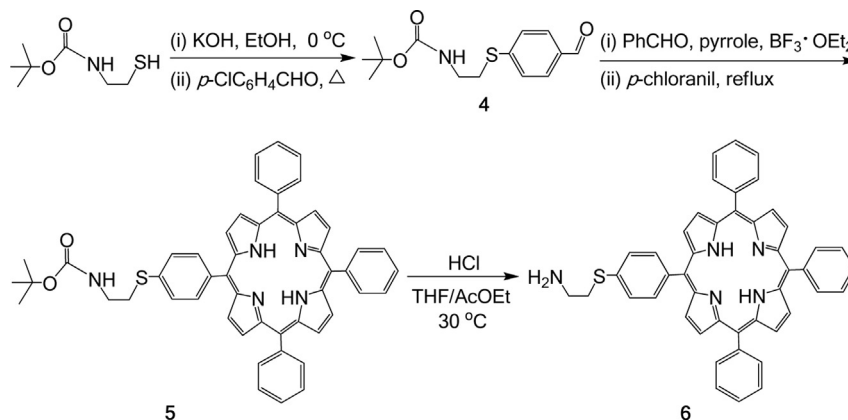
and  $[(\mu\text{-SCH}_2)_2\text{NCH}(\text{CO}_2\text{Et})\text{CH}_2\text{SFe}(\text{CO})_2\text{Cp}]\text{Fe}_2(\text{CO})_5$  (2.299 Å) [49]. Finally, it is interesting to note that the coordination mode of the porphyrinylthioether with diiron subsite in **8** is very similar to that of the  $[\text{Fe}_4\text{S}_4]$  cluster and  $[\text{Fe}_2\text{S}_2]$  cluster in the natural enzymes.

### 3. Experimental section

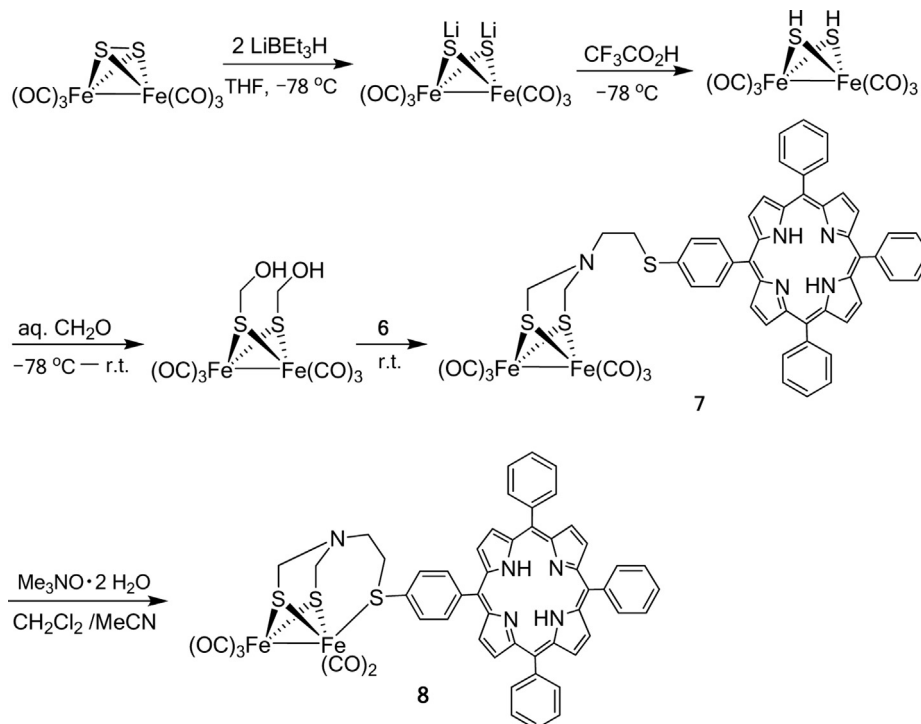
All reactions were performed using standard Schlenk and vacuum-line techniques under an atmosphere of nitrogen. Dichloromethane was distilled under  $\text{N}_2$  over  $\text{CaH}_2$ , absolute ethanol from freshly prepared magnesium ethoxide, THF from sodium/benzophenone ketyl, and MeCN once from  $\text{P}_2\text{O}_5$  and then from  $\text{CaH}_2$ . While Boc-NHC<sub>2</sub>H<sub>4</sub>SH [50],  $(\mu\text{-S}_2)\text{Fe}_2(\text{CO})_6$  [51] and  $(\mu\text{-SCH}_2)_2\text{CH}(\text{OH})\text{Fe}_2(\text{CO})_6$  [44] were prepared according to literature procedures,  $\text{LiBEt}_3\text{H}$  (1 M in THF),  $\text{Me}_3\text{NO}\cdot 2\text{H}_2\text{O}$ ,  $\text{BF}_3\cdot \text{OEt}_2$ , pyrrole, benzaldehyde, 2,3,5,6-tetrachlorobenzoquinone (*p*-chloranil),  $\text{CF}_3\text{CO}_2\text{H}$ , *p*-CHOC<sub>6</sub>H<sub>4</sub>CO<sub>2</sub>H, and *p*-ClC<sub>6</sub>H<sub>4</sub>CHO were of commercial origin. Preparative TLC was carried out on glass plates (26 × 20 × 0.25 cm) coated with silica gel H (10–40 μm) or fluorescence silica gel GF254 (10–40 μm). IR spectra were recorded on a Bruker Vector 22 infrared spectrophotometer. UV–vis spectra were taken on a Varian CARY 100 Bio spectrophotometer. <sup>1</sup>H NMR spectra were recorded on a Varian Mercury Plus 400 NMR spectrometer. Elemental analyses were performed on an Elementar Vario EL analyzer. Melting points were determined on a Yanaco MP-500 apparatus and are uncorrected.

#### 3.1. Preparation of $[(\mu\text{-SCH}_2)_2\text{CHO}_2\text{CC}_6\text{H}_4\text{CHO-}p]\text{Fe}_2(\text{CO})_6$ (**1**)

To a stirred suspension of *p*-CHOC<sub>6</sub>H<sub>4</sub>CO<sub>2</sub>H (0.30 g, 2.0 mmol) in benzene (10 mL) was added  $\text{SOCl}_2$  (0.6 mL, 8.0 mmol) and then the mixture was refluxed for 3 h. Solvent was removed at reduced pressure to give the corresponding acid chloride *p*-CHOC<sub>6</sub>H<sub>4</sub>COCl, which was dissolved in  $\text{CH}_2\text{Cl}_2$  (10 mL). To this solution was added  $\text{Et}_3\text{N}$  (0.4 mL, 2.0 mmol) and then the mixture was treated at 0 °C dropwise with a solution of  $[(\mu\text{-SCH}_2)_2\text{CH}(\text{OH})]\text{Fe}_2(\text{CO})_6$  (0.80 g, 2.0 mmol) in  $\text{CH}_2\text{Cl}_2$  (60 mL). After the new mixture was stirred at room temperature for 2 h, it was washed three times with water (20 × 3 mL). The separated organic layers were combined and dried over anhydrous  $\text{Na}_2\text{SO}_4$ . After  $\text{Na}_2\text{SO}_4$  and solvent were removed, the residue was subjected to TLC separation using petroleum ether/ $\text{CH}_2\text{Cl}_2$  (2:1 = v/v) as eluent. From the major red band, **1** was obtained as a red solid (0.662 g, 62%), m.p. 162–164 °C. Anal. Calcd for  $\text{C}_{17}\text{H}_{10}\text{Fe}_2\text{O}_9\text{S}_2$ : C, 38.27; H, 1.89. Found: C, 38.22; H, 1.84. IR (KBr disk):  $\nu_{\text{C}\equiv\text{O}}$  2075 (s), 2035 (vs), 2018 (vs), 1992 (vs);  $\nu_{\text{C}=\text{O}}$  1706 (s)  $\text{cm}^{-1}$ . <sup>1</sup>H NMR (400 MHz,  $\text{CDCl}_3$ ):  $\delta$  = 1.72 (t, 2H<sub>a</sub>,  $J_{\text{HaHa}'} = J_{\text{HaHa}''} = 12.0$  Hz), 2.92–2.96 (m, 2H<sub>e</sub>), 4.50 (br. s, 1H<sub>a'</sub>), 7.92 (d, 2H,  $J = 7.6$  Hz,



Scheme 2. Synthetic routes of **4–6**.

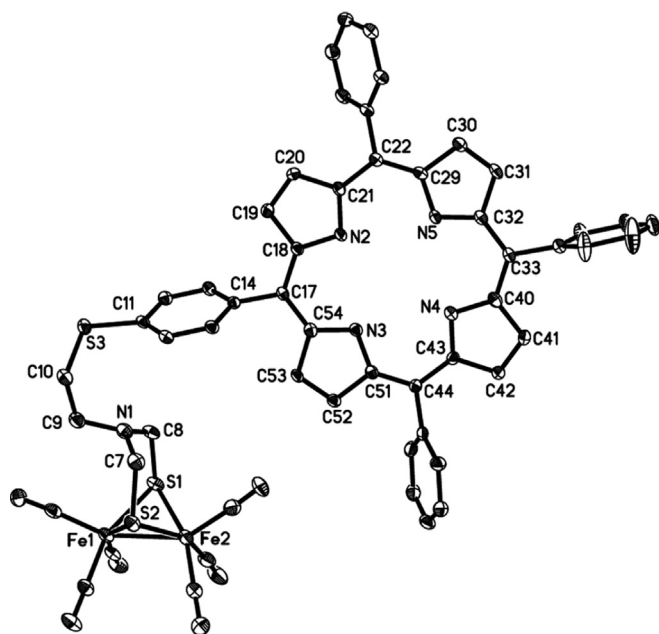
Scheme 3. Synthetic routes of **7** and **8**.

2*m*-H of C<sub>6</sub>H<sub>4</sub>CHO), 8.10 (d, 2H, *J* = 7.6 Hz, 2*o*-H of C<sub>6</sub>H<sub>4</sub>CHO), 10.09 (s, 1H, CHO) ppm (In this paper H<sub>a</sub> and H<sub>e</sub> denote the axially and equatorially bonded H atoms in CH<sub>2</sub>S groups, while H<sub>a'</sub> represents that axially bonded to bridgehead C atom).

### 3.2. Preparation of 5-[*p*-Fe<sub>2</sub>(CO)<sub>6</sub>(μ-SCH<sub>2</sub>)<sub>2</sub>CHO<sub>2</sub>C<sub>6</sub>H<sub>4</sub>],10,15,20-triphenylporphyrin (**2**)

To a stirred solution of **1** (0.437 g, 0.82 mmol), benzaldehyde (0.25 mL, 2.46 mmol) in CHCl<sub>3</sub> (300 mL) was added pyrrole (0.23 mL, 3.28 mmol). After the mixture was stirred in the dark for 15 min

BF<sub>3</sub>·OEt<sub>2</sub> (0.041 mL, 0.33 mmol) was added. After the new mixture was stirred in the dark for 15 h, 2,3,5,6-tetrachlorobenzoquinone (*p*-chloranil) (0.80 g, 3.28 mmol) was added. The mixture refluxed in the dark for 1.5 h and then was cooled to room temperature. After the mixture was concentrated to about 1/3 volume at reduced pressure, the residue was subjected to flash column chromatography (Al<sub>2</sub>O<sub>3</sub>, CH<sub>2</sub>Cl<sub>2</sub>) and then the eluate was concentrated to a suitable volume for TLC separation. From the first purple band using CH<sub>2</sub>Cl<sub>2</sub>/petroleum ether (1:2 = v/v) as eluent, TPP (0.098 g, 18%) was obtained as a purple solid, which was identified by comparison of its IR and <sup>1</sup>H NMR spectra with those of the authentic sample [40,41]. From the second purple band using CH<sub>2</sub>Cl<sub>2</sub>/petroleum ether (1:1 v/v) as eluent, **2** (0.178 g, 21%) as a purple solid was obtained. m.p. 174 °C (dec). Anal. Calcd for C<sub>54</sub>H<sub>34</sub>Fe<sub>2</sub>N<sub>4</sub>O<sub>8</sub>S<sub>2</sub>: C, 62.20; H, 3.29; N, 5.37. Found: C, 61.96; H, 3.28; N, 5.35. IR (KBr disk): ν<sub>C≡O</sub> 2075 (s), 2035 (vs), 1998 (vs); ν<sub>C=O</sub> 1722 (s); ν<sub>pyrrole rings</sub> 1558 (m), 1473 (m), 1344 (m) cm<sup>-1</sup>. <sup>1</sup>H NMR (300 MHz, CDCl<sub>3</sub>): δ = -2.80 (s, 2H, 2NH of pyrrole rings), 1.86 (t, 2H<sub>a</sub>, *J*<sub>HaHe</sub> = *J*<sub>HaHa'</sub> = 12.2 Hz), 3.11 (dd, 2H<sub>e</sub>, *J*<sub>HeHa</sub> = 12.6 Hz, *J*<sub>HeHa'</sub> = 4.2 Hz), 4.63–4.73 (m, 1H<sub>a'</sub>), 7.73–7.78 (m, 9H, 6 *m*-H of 3C<sub>6</sub>H<sub>5</sub>, 3 *p*-H of 3C<sub>6</sub>H<sub>5</sub>), 8.19–8.23 (m, 6H, 6 *o*-H of 3C<sub>6</sub>H<sub>5</sub>), 8.29, 8.34 (dd, 4H, AB system, *J* = 8.4 Hz, C<sub>6</sub>H<sub>4</sub>), 8.72–8.85 (m, 8H, 8CH of pyrrole rings) ppm. UV–vis (CH<sub>2</sub>Cl<sub>2</sub>): λ<sub>max</sub> (log ε) = 412 (5.09), 514 (4.27), 549 (3.90), 589 (3.73), 645 (3.59) nm.

Fig. 6. ORTEP view of **7** with 30% probability level ellipsoids.Table 4  
Selected bond lengths (Å) and angles (°) for **7**.

Bond lengths			
Fe(1)–S(1)	2.2671(14)	Fe(1)–Fe(2)	2.5109(11)
Fe(1)–S(2)	2.2673(14)	Fe(2)–S(1)	2.2637(15)
S(1)–C(8)	1.874(4)	Fe(2)–S(2)	2.2524(15)
S(2)–C(7)	1.865(4)	S(3)–C(11)	1.786(4)
Bond angles			
S(1)–Fe(1)–S(2)	84.52(5)	C(8)–S(1)–Fe(2)	110.42(17)
S(1)–Fe(1)–Fe(2)	56.28(4)	N(1)–C(9)–C(10)	111.6(4)
Fe(1)–S(1)–Fe(2)	67.31(4)	C(9)–C(10)–S(3)	115.6(3)
C(8)–S(1)–Fe(1)	112.13(16)	C(11)–S(3)–C(10)	107.2(2)

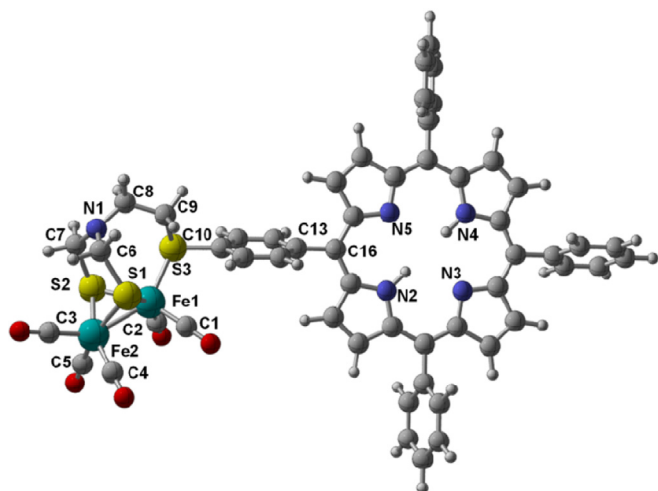


Fig. 7. Fully optimized structure of **8**. The gray, cyan, red, yellow, blue and pale balls denote carbon, iron, oxygen, sulfur, nitrogen, and hydrogen atoms, respectively. (For interpretation of the references to color in this figure legend, the reader is referred to the web version of this article.)

### 3.3. Preparation of 5-[*p*-Fe<sub>2</sub>(CO)<sub>6</sub>(μ-SCH<sub>2</sub>)<sub>2</sub>CHO<sub>2</sub>CC<sub>6</sub>H<sub>4</sub>],10,15,20-triphenylporphyrinozinc (**3**)

To a solution of **2** (0.042 g, 0.04 mmol) in CHCl<sub>3</sub> (20 mL) was added a MeOH solution (2 mL) of Zn(OAc)<sub>2</sub>·2H<sub>2</sub>O (0.57 g, 0.26 mmol). After the mixture was refluxed for 2 h and then cooled to room temperature, the resulting mixture was filtered and the filtrate was sequentially washed using an aqueous solution saturated with NaHCO<sub>3</sub> and NaCl. The separated organic layers were combined and dried with anhydrous MgSO<sub>4</sub>. After removal of MgSO<sub>4</sub>, volatiles were evaporated under vacuum and the residue was subjected to TLC using CH<sub>2</sub>Cl<sub>2</sub>/petroleum ether (3:2 = v/v) as eluent. From the main band, **3** (0.039 g, 88%) was obtained as a purple solid, m.p. 196 °C (dec). Anal. Calcd for C<sub>54</sub>H<sub>32</sub>Fe<sub>2</sub>N<sub>4</sub>O<sub>8</sub>S<sub>2</sub>Zn: C 58.64; H, 2.92; N, 5.07. Found: C, 58.41; H, 2.68; N, 5.17. IR (KBr disk): ν<sub>C≡O</sub> 2075 (s), 2036 (vs), 2000 (vs); ν<sub>C=O</sub> 1720 (s); ν<sub>pyrrole rings</sub> 1558 (m), 1487 (m), 1339 (m) cm<sup>-1</sup>. <sup>1</sup>H NMR (400 MHz, CDCl<sub>3</sub>): δ = 1.86 (t, 2H<sub>a</sub>, J<sub>HaHe</sub> = J<sub>HaHa'</sub> = 12.2 Hz), 3.11 (dd, 2H<sub>e</sub>, J<sub>HeHa</sub> = 12.8 Hz, J<sub>HeHa'</sub> = 4.0 Hz), 4.64–4.72 (m, 1H<sub>a'</sub>), 7.73–7.78 (m, 9H, 6 *m*-H of 3C<sub>6</sub>H<sub>5</sub>, 3 *p*-H of 3C<sub>6</sub>H<sub>5</sub>), 8.19–8.23 (m, 6H, 6 *o*-H of 3C<sub>6</sub>H<sub>5</sub>), 8.28, 8.35 (dd, 4H, AB system, J = 8.0 Hz, C<sub>6</sub>H<sub>4</sub>), 8.82–8.97 (m, 8H, 8CH of pyrrole rings) ppm. UV–vis (CH<sub>2</sub>Cl<sub>2</sub>): λ<sub>max</sub> (log ε) = 414 (5.08), 548 (4.46), 586 (3.57) nm.

Table 5

Selected bond lengths (Å) and angles (°) for **8** based on BP86/6-311+G\*\* geometry.

Bond lengths			
Fe(1)–S(1)	2.312	Fe(1)–Fe(2)	2.533
Fe(1)–S(2)	2.300	Fe(2)–S(1)	2.308
Fe(1)–S(3)	2.275	Fe(2)–S(2)	2.306
S(1)–C(6)	1.908	N(1)–C(6)	1.427
S(2)–C(7)	1.900	N(1)–C(7)	1.431
S(3)–C(9)	1.858	N(1)–C(8)	1.463
S(3)–C(10)	1.814	C(13)–C(16)	1.500
Bond angles			
S(1)–Fe(1)–S(2)	85.84	C(10)–S(3)–Fe(1)	113.01
S(1)–Fe(2)–S(2)	85.81	C(9)–S(3)–Fe(1)	109.08
S(1)–Fe(1)–Fe(2)	56.67	C(9)–S(3)–C(10)	100.01
S(2)–Fe(1)–Fe(2)	56.74	S(3)–Fe(1)–C(1)	103.97
S(1)–Fe(2)–Fe(1)	56.83	C(6)–N(1)–C(7)	115.38
S(2)–Fe(2)–Fe(1)	56.54	C(6)–S(1)–Fe(1)	111.78
Fe(1)–S(1)–Fe(2)	66.50	C(7)–S(2)–Fe(2)	110.08
Fe(1)–S(2)–Fe(2)	66.73	C(8)–C(9)–S(3)	111.80

### 3.4. Preparation of *p*-Boc-NHC<sub>2</sub>H<sub>4</sub>SC<sub>6</sub>H<sub>4</sub>CHO (**4**)

A solution of KOH (1.13 g, 20.2 mmol) in EtOH (25 mL) at 0 °C was treated dropwise with a solution of Boc-NHC<sub>2</sub>H<sub>4</sub>SH (3.54 g, 20.0 mmol) in EtOH (5 mL). After the mixture was stirred at 0 °C for 30 min, *p*-ClC<sub>6</sub>H<sub>4</sub>CHO (2.70 g, 19.2 mmol) was added, and then the new mixture was stirred at 75–78 °C for 3 h, resulting in a pale yellow solution with some KCl precipitates. To this mixture was added water (70 mL), and then the resulting solution was extracted with CCl<sub>4</sub> (20 mL × 4). After CCl<sub>4</sub> was removed from the extracts in vacuum, the residue was subjected to fluorescence TLC separation using acetone/petroleum ether (1:5 = v/v) as eluent. From the major band, **4** was obtained as a white solid (2.69 g, 50%), m.p. 51–52 °C. Anal. Calcd for C<sub>14</sub>H<sub>19</sub>NO<sub>3</sub>S: C, 59.76; H, 6.81; N, 4.98. Found: C, 59.70; H, 6.70; N, 5.07. IR (KBr disk): ν<sub>C=O</sub> 1691 (vs), 1682 (s) cm<sup>-1</sup>. <sup>1</sup>H NMR (400 MHz, CDCl<sub>3</sub>): δ = 1.44 (s, 9H, C(CH<sub>3</sub>)<sub>3</sub>), 3.17 (t, 2H, J = 6.4 Hz, NCH<sub>2</sub>CH<sub>2</sub>S), 3.40, 3.42 (2s, 2H, NCH<sub>2</sub>CH<sub>2</sub>S), 4.90 (s, 1H, NH), 7.42 (d, 2H, J = 8.0 Hz, 2*m*-H of C<sub>6</sub>H<sub>4</sub>CHO), 7.78 (d, 2H, J = 8.4 Hz, 2*o*-H of C<sub>6</sub>H<sub>4</sub>CHO), 9.93 (s, 1H, CHO) ppm.

### 3.5. Preparation of 5-(*p*-Boc-NHC<sub>2</sub>H<sub>4</sub>SC<sub>6</sub>H<sub>4</sub>),10,15,20-triphenylporphyrin (**5**)

A solution of **4** (0.30 g, 1.1 mmol), pyrrole (0.28 mL, 4.0 mmol), PhCHO (0.30 mL, 3.0 mmol), and BF<sub>3</sub>·OEt<sub>2</sub> (0.05 mL, 0.40 mmol) in CH<sub>2</sub>Cl<sub>2</sub> (400 mL) was stirred in the dark at room temperature for 16 h to give a purple solution. To this solution was added *p*-chloranil (0.984 g, 4.0 mmol), and then the new mixture was heated at reflux for 2 h to give a brown solution. After solvent was removed at reduced pressure, the residue was subjected to flash column chromatography (Al<sub>2</sub>O<sub>3</sub>, CH<sub>2</sub>Cl<sub>2</sub>). The eluate was reduced to a suitable volume for TLC separation by using CH<sub>2</sub>Cl<sub>2</sub>/petroleum ether (12:1 = v/v) as eluent. From the first purple band, TPP (0.115 g, 25%) was obtained as a purple solid, which was identified by comparison of its IR and <sup>1</sup>H NMR spectra with those of the authentic sample [40,41]. From the second purple-red band, **5** was obtained as a purple solid (0.154 g, 20%), m.p. 244–246 °C. Anal. Calcd for C<sub>51</sub>H<sub>43</sub>N<sub>5</sub>O<sub>2</sub>S: C, 77.54; H, 5.49; N, 8.87. Found: C, 77.42; H, 5.52; N, 8.91. IR (KBr disk): ν<sub>C=O</sub> 1715 (vs); ν<sub>pyrrole rings</sub> 1558 (m), 1473 (s), 1349 (m) cm<sup>-1</sup>. <sup>1</sup>H NMR (400 MHz, CDCl<sub>3</sub>): δ = -2.78 (s, 2H, 2NH of pyrrole rings), 1.49 (s, 9H, C(CH<sub>3</sub>)<sub>3</sub>), 3.31 (t, 2H, J = 6.0 Hz, NCH<sub>2</sub>CH<sub>2</sub>S), 3.58, 3.59 (2s, 2H, NCH<sub>2</sub>CH<sub>2</sub>S), 5.09 (s, 1H, Boc-NH), 7.70–7.75 (m, 11H, 2*o*-H of SC<sub>6</sub>H<sub>4</sub>, 6*m*-H of 3C<sub>6</sub>H<sub>5</sub>, 3*p*-H of 3C<sub>6</sub>H<sub>5</sub>), 8.13, 8.14 (2s, 2H, 2*m*-H of SC<sub>6</sub>H<sub>4</sub>), 8.20, 8.22 (2s, 6H, 6*o*-H of 3C<sub>6</sub>H<sub>5</sub>), 8.85 (s, 8H, 8CH of pyrrole rings) ppm.

### 3.6. Preparation of 5-(*p*-NH<sub>2</sub>C<sub>2</sub>H<sub>4</sub>SC<sub>6</sub>H<sub>4</sub>),10,15,20-triphenylporphyrin (**6**)

To a solution of HCl (2 mol L<sup>-1</sup>) in THF/ethyl acetate (20 mL, 1:1 in volume) was added **5** (0.166 g, 0.21 mmol), and then the mixture was stirred at 30 °C for about 2 h. After volatiles were removed at reduced pressure, the green residue was redissolved in CHCl<sub>3</sub> (40 mL) and washed sequentially with saturated aqueous NaHCO<sub>3</sub> (40 mL) and aqueous NaCl (10 mL). After CHCl<sub>3</sub> was removed at reduced pressure, the purple residue was subjected to TLC separation using CH<sub>2</sub>Cl<sub>2</sub>/ethanol (10:1 = v/v) as eluent to give **6** as a purple solid (0.125 g, 86%), m.p. 196 °C (dec). Anal. Calcd for C<sub>46</sub>H<sub>35</sub>N<sub>5</sub>S: C, 80.09; H, 5.11; N, 10.15. Found: C, 79.98; H, 5.19; N, 10.09. IR (KBr disk): ν<sub>pyrrole rings</sub> 1558 (m), 1472 (s), 1349 (m) cm<sup>-1</sup>. <sup>1</sup>H NMR (400 MHz, CDCl<sub>3</sub>): δ = -2.77 (s, 2H, 2 NH of pyrrole rings), 2.50 (br s, 2H, NH<sub>2</sub>), 3.22, 3.24 (2s, 2H, NCH<sub>2</sub>CH<sub>2</sub>S), 3.33 (t, 2H, J = 5.6 Hz, NCH<sub>2</sub>CH<sub>2</sub>S), 7.70–7.78 (m, 11H, 2*o*-H of SC<sub>6</sub>H<sub>4</sub>, 6*m*-H of 3C<sub>6</sub>H<sub>5</sub>, 3*p*-H of 3C<sub>6</sub>H<sub>5</sub>), 8.13, 8.15 (2s, 2H, 2*m*-H of SC<sub>6</sub>H<sub>4</sub>), 8.23 (s, 6H, 6*o*-H of 3C<sub>6</sub>H<sub>5</sub>), 8.87 (s, 8H, 8CH of pyrrole rings) ppm.

**Table 6**  
Crystal data and structure refinements details for **1–3** and **7**.

	<b>1</b>	<b>2</b>	<b>3</b>	<b>7</b>
Formula	C <sub>17</sub> H <sub>10</sub> Fe <sub>2</sub> O <sub>9</sub> S <sub>2</sub>	C <sub>54</sub> H <sub>34</sub> Fe <sub>2</sub> N <sub>4</sub> O <sub>8</sub> S <sub>2</sub> ·2CH <sub>2</sub> Cl	C <sub>54</sub> H <sub>32</sub> Fe <sub>2</sub> N <sub>4</sub> O <sub>8</sub> S <sub>2</sub> Zn·2CH <sub>3</sub> OH·1.5o-Cl <sub>2</sub> C <sub>6</sub> H <sub>4</sub>	C <sub>54</sub> H <sub>37</sub> Fe <sub>2</sub> N <sub>5</sub> O <sub>6</sub> S <sub>3</sub>
Formula weight	534.07	1127.60	1390.60	1059.77
Crystal syst	Triclinic	Monoclinic	Monoclinic	Triclinic
Space group	P $\bar{1}$	P121/a1	P $\bar{1}$	P $\bar{1}$
<i>a</i> (Å)	7.5740(10)	12.8588(10)	9.724(4)	10.640(4)
<i>b</i> (Å)	8.8550(14)	8.9807(6)	13.185(5)	12.649(4)
<i>c</i> (Å)	16.512(2)	43.103(3)	23.990(9)	17.847(6)
$\alpha$ (°)	92.697(7)	90	93.391(2)	94.988(6)
$\beta$ (°)	93.435(6)	96.443(4)	94.266(4)	92.298(6)
$\gamma$ (°)	110.481(8)	90	98.248(7)	91.862(7)
<i>V</i> (Å <sup>3</sup> )	1032.8(3)	4946.1(6)	3028(2)	2389.3(14)
<i>Z</i>	2	4	2	2
<i>D<sub>c</sub></i> (g cm <sup>-3</sup> )	1.717	1.514	1.524	1.473
$\mu$ (Mo-K $\alpha$ ) (mm <sup>-1</sup> )	1.653	0.841	1.131	0.796
<i>F</i> (000)	536.00	2304	1418	1088
Limiting indices	-9 ≤ <i>h</i> ≤ 9 -7 ≤ <i>k</i> ≤ 11 -21 ≤ <i>l</i> ≤ 21	-15 ≤ <i>h</i> ≤ 14 -10 ≤ <i>k</i> ≤ 10 -51 ≤ <i>l</i> ≤ 51	-11 ≤ <i>h</i> ≤ 11 -15 ≤ <i>k</i> ≤ 15 -28 ≤ <i>l</i> ≤ 28	-12 ≤ <i>h</i> ≤ 12 -15 ≤ <i>k</i> ≤ 15 -19 ≤ <i>l</i> ≤ 21
No. of rflns	7869	32,173	22,946	24,718
No. of indep rflns	4826	8572	10,480	8409
2 $\theta$ <sub>max</sub> (°)	55.74	50.00	50.04	50.02
<i>R</i>	0.0316	0.0749	0.0934	0.0664
<i>R<sub>w</sub></i>	0.0738	0.1718	0.1978	0.1589
Goodness-of-fit	0.955	1.160	1.102	1.102
Largest diff peak and hole (e Å <sup>-3</sup> )	0.311/-0.424	0.415/-1.135	1.059/-1.242	0.529/-0.431

### 3.7. Preparation of 5-[*p*-Fe<sub>2</sub>(CO)<sub>6</sub>( $\mu$ -SCH<sub>2</sub>)<sub>2</sub>NC<sub>2</sub>H<sub>4</sub>SC<sub>6</sub>H<sub>4</sub>],10,15,20-triphenylporphyrin] (**7**)

A red solution of ( $\mu$ -S)<sub>2</sub>Fe<sub>2</sub>(CO)<sub>6</sub> (0.034 g, 0.10 mmol) in THF (10 mL) was cooled to -78 °C, and then treated dropwise with Et<sub>3</sub>BHLi (0.20 mL, 0.20 mmol) to give a green solution containing ( $\mu$ -LiS)<sub>2</sub>Fe<sub>2</sub>(CO)<sub>6</sub>. After stirring for 15 min, CF<sub>3</sub>CO<sub>2</sub>H (0.016 mL, 0.20 mmol) was added to cause an immediate color change from green to red, indicating the complete conversion of ( $\mu$ -LiS)<sub>2</sub>Fe<sub>2</sub>(CO)<sub>6</sub> to ( $\mu$ -HS)<sub>2</sub>Fe<sub>2</sub>(CO)<sub>6</sub>. After the mixture was stirred for an additional 10 min at -78 °C, 40% aqueous formaldehyde (0.017 mL, 0.20 mmol) was added. The new mixture was allowed to warm to room temperature and stirred at this temperature for 1 h to give ( $\mu$ -HOCH<sub>2</sub>S)<sub>2</sub>Fe<sub>2</sub>(CO)<sub>6</sub>. After **6** (0.055 g, 0.08 mmol) was added, the mixture was stirred at room temperature for 1.5 h. Solvent was removed in vacuum and the residue was subjected to TLC separation using CH<sub>2</sub>Cl<sub>2</sub>/petroleum ether (1:1 = v/v) as eluent. From the purple band, **7** (0.043 g, 51%) was obtained as a purple-red solid, m.p. 175 °C (dec). Anal. Calcd for C<sub>54</sub>H<sub>37</sub>Fe<sub>2</sub>N<sub>5</sub>O<sub>6</sub>S<sub>3</sub>: C, 61.20; H, 3.52; N, 6.61. Found: C, 60.98; H, 3.78; N, 6.51. IR (KBr disk):  $\nu_{\text{C}\equiv\text{O}}$  2070 (s), 2027 (vs), 1989 (vs), 1958 (s);  $\nu_{\text{pyrrole rings}}$  1558 (m), 1473 (s), 1348 (m) cm<sup>-1</sup>. <sup>1</sup>H NMR (400 MHz, CDCl<sub>3</sub>):  $\delta$  = -2.76 (s, 2H, 2NH of pyrrole rings), 3.10 (t, 2H, *J* = 6.8 Hz, NCH<sub>2</sub>CH<sub>2</sub>S), 3.23 (t, 2H, *J* = 7.0 Hz, NCH<sub>2</sub>CH<sub>2</sub>S), 3.76 (s, 4H, N(CH<sub>2</sub>S)<sub>2</sub>), 7.64, 7.66 (2s, 2H, 2o-H of SC<sub>6</sub>H<sub>4</sub>), 7.75–7.80 (m, 9H, 6*m*-H of 3C<sub>6</sub>H<sub>5</sub>, 3*p*-H of 3C<sub>6</sub>H<sub>5</sub>) 8.15, 8.17 (2s, 2H, 2*m*-H of SC<sub>6</sub>H<sub>4</sub>), 8.22, 8.24 (2s, 6H, 6o-H of 3C<sub>6</sub>H<sub>5</sub>), 8.80–8.88 (m, 8H, 8CH of pyrrole rings) ppm. UV–vis (CH<sub>2</sub>Cl<sub>2</sub>):  $\lambda_{\text{max}}$  (log  $\epsilon$ ) = 418 (4.65), 515 (3.35), 550 (3.07), 591 (2.90), 645 (2.80) nm.

### 3.8. Preparation of 5-[*p*-Fe<sub>2</sub>(CO)<sub>5</sub>( $\mu$ -SCH<sub>2</sub>)<sub>2</sub>NC<sub>2</sub>H<sub>4</sub>SC<sub>6</sub>H<sub>4</sub>],10,15,20-triphenylporphyrin] (**8**)

To a solution of **7** (0.012 g, 0.011 mmol) in CH<sub>2</sub>Cl<sub>2</sub> was added a solution of Me<sub>3</sub>NO·2H<sub>2</sub>O (0.002 g, 0.018 mmol) in MeCN (5 mL). After the mixture was stirred at room temperature for 4 h, solvents were removed and the residue was subjected to TLC separation using CH<sub>2</sub>Cl<sub>2</sub>/petroleum ether (1:1 = v/v) as eluent. From the main

band, **8** (0.010 g, 88%) was obtained as a purple–red solid, m.p. 148 °C (dec). Anal. Calcd for C<sub>53</sub>H<sub>37</sub>Fe<sub>2</sub>N<sub>5</sub>O<sub>5</sub>S<sub>3</sub>: C, 61.70; H, 3.61; N, 6.79. Found: C, 61.61; H, 3.71; N, 6.75. IR (KBr disk):  $\nu_{\text{C}\equiv\text{O}}$  2070 (s), 2044 (vs), 2032 (vs), 1984 (vs), 1935 (m);  $\nu_{\text{pyrrole rings}}$  1558 (m), 1472 (s), 1349 (m) cm<sup>-1</sup>. <sup>1</sup>H NMR (400 MHz, CDCl<sub>3</sub>):  $\delta$  = -2.77 (s, 2H, 2NH of pyrrole rings), 3.29 (s, 2H, NCH<sub>2</sub>CH<sub>2</sub>S), 3.68 (s, 2H, NCH<sub>2</sub>CH<sub>2</sub>S), 4.11 (s, 4H, N(CH<sub>2</sub>S)<sub>2</sub>), 7.76, 7.78 (2s, 9H, 6*m*-H of 3C<sub>6</sub>H<sub>5</sub>, 3*p*-H of 3C<sub>6</sub>H<sub>5</sub>) 8.18–8.23 (m, 8H, 2o-H of SC<sub>6</sub>H<sub>4</sub>, 6o-H of 3C<sub>6</sub>H<sub>5</sub>), 8.36, 8.38 (2s, 2H, 2*m*-H of SC<sub>6</sub>H<sub>4</sub>), 8.83–8.90 (m, 8H, 8CH of pyrrole rings) ppm. UV–vis (CH<sub>2</sub>Cl<sub>2</sub>):  $\lambda_{\text{max}}$  (log  $\epsilon$ ) = 418 (4.59), 514 (3.33), 550 (3.08), 591 (2.93), 645 (2.84) nm.

### 3.9. X-ray structure determinations of **1–3** and **7**

Single crystals of **1–3** and **7** suitable for X-ray diffraction analyses were grown by slow evaporation of the CH<sub>2</sub>Cl<sub>2</sub>/hexane solution of **1** at -20 °C, as well as by slow diffusion of hexane to the CH<sub>2</sub>Cl<sub>2</sub> solution of **2**, slow diffusion of MeOH to the o-Cl<sub>2</sub>C<sub>6</sub>H<sub>4</sub> solution of **3**, and slow diffusion of MeOH to the CH<sub>2</sub>Cl<sub>2</sub> solution of **7** at room temperature, respectively. All the single crystals were mounted on a Rigaku MM-007 (rotating anode) diffractometer equipped with a Saturn 70 CCD. Data were collected at room temperature, using a confocal monochromator with MoK $\alpha$  radiation ( $\lambda$  = 0.71070 Å) in the  $\omega$ - $\phi$  scanning mode. Data collection, reduction, and absorption correction were performed with the CRYSTALCLEAR program [52]. The structures were solved by direct methods using the SHELXS-97 program [53] and refined by full-matrix least-squares techniques (SHELXL-97) [54] on *F*<sup>2</sup>. Hydrogen atoms were located by using the geometric method. Details of crystal data, data collections, and structure refinements are summarized in Table 6.

### 3.10. Computational methods

Full geometry optimizations were carried out at the BP86/6-311+G\*\* level of theory, and the optimized structure was characterized as local minima by frequency analysis at the same level of theory. All the computations were performed with the Gaussian 09 program [55].

#### 4. Conclusion

On the basis of preparing the corresponding precursors **1** and **4–6**, we have synthesized the first porphyrinylester moiety- and porphyrinylthioether moiety-containing model complexes **2**, **3**, **7**, and **8**. While the porphyrin macrocycle-containing model complex **2** can be prepared by the porphyrin macrocycle formation reaction of the simple *p*-formylbenzoate functionalized model complex **1** with PhCHO, pyrrole, BF<sub>3</sub>·OEt<sub>2</sub>, and *p*-chloranil, the porphyrinozinc macrocycle-containing model complex **3** is prepared by coordination reaction of **2** with Zn(OAc)<sub>2</sub>. In addition, model complex **7** can be prepared by in situ condensation/cyclization reaction of (μ-HOCH<sub>2</sub>S)<sub>2</sub>Fe<sub>2</sub>(CO)<sub>6</sub> with *p*-aminoethylthio-substituted tetraphenylporphyrin **6**, whereas the Me<sub>3</sub>NO-assisted CO substitution reaction of **7** results in formation of model complex **8**. All these new compounds **1–8** have been characterized by elemental analysis and various spectroscopic techniques. Particularly noteworthy is that the X-ray crystallography confirms that **7** has a pendent porphyrinylthioether moiety that is attached to its bridgehead N atom, whereas DFT computations reveal that the porphyrinylthioether moiety in **8** is coordinated via its S atom to one Fe atom in its diiron-ADT subsite.

#### Acknowledgments

Financial support in China by the State Key Project of Fundamental Research for Nanoscience and Nanotechnology (973) (Grant number 2011CB935902), the National Natural Science Foundation of China (Grant numbers 21132001, 21272122), Synergetic Innovation Center of Chemical Science and Engineering (Tianjin), and in USA by Department of Defense (Grant number W911NF-12-1-0083) and NSF (Grant number EPS-1010094), is gratefully acknowledged.

#### Appendix A. Supplementary material

CCDC 929066 for **1**, 929067 for **2**, 929068 for **3** and 899092 for **7** contain the supplementary crystallographic data for this paper. These data can be obtained free of charge from The Cambridge Crystallographic Data Centre via [www.ccdc.cam.ac.uk/data\\_request/cif](http://www.ccdc.cam.ac.uk/data_request/cif).

#### Appendix B. Supplementary data

Supplementary data related to this article can be found at <http://dx.doi.org/10.1016/j.jorganchem.2013.09.007>.

#### References

- (a) M.W.W. Adams, E.I. Stiefel, *Science* 282 (1998) 1842–1843; (b) R. Cammack, *Nature* 397 (1999) 214–215.
- Y. Nicolet, B.J. Lemon, J.C. Fontecilla-Camps, J.W. Peters, *Trends Biochem. Sci.* 25 (2000) 138–143.
- A.E. Przybyla, J. Robbins, N. Menon, H.D. Peck, *FEMS Microbiol. Lett.* 88 (1992) 109–135.
- A. Volbeda, L. Martin, C. Cavazza, M. Matho, B.W. Faber, W. Roseboom, S.P.J. Albracht, E. Garcin, M. Rousset, J.C. Fontecilla-Camps, *J. Biol. Inorg. Chem.* 10 (2005) 239–249.
- A. Volbeda, J.C. Fontecilla-Camps, *Dalton Trans.* (2003) 4030–4038.
- E. Garcin, X. Vernède, E.C. Hatchikian, A. Volbeda, M. Frey, J.C. Fontecilla-Camps, *Structure* 7 (1999) 557–566.
- E.J. Lyon, S. Shima, G. Buurman, S. Chowdhuri, A. Batschauer, K. Steinbach, R.K. Thauer, *Eur. J. Biochem.* 271 (2004) 195–204.
- S. Shima, R.K. Thauer, *Chem. Rec.* 7 (2007) 37–46.
- M.W.W. Adams, *Biochim. Biophys. Acta* 1020 (1990) 115–145.
- M. Frey, *ChemBioChem* 3 (2002) 153–160.
- D.J. Evans, C.J. Pickett, *Chem. Soc. Rev.* 32 (2003) 268–275.
- W. Lubitz, B. Tumas, *Chem. Rev.* 107 (2007) 3900–3903.
- J. Alper, *Science* 299 (2003) 1686–1687.
- J.W. Peters, W.N. Lanzilotta, B.J. Lemon, L.C. Seefeldt, *Science* 282 (1998) 1853–1858.
- Y. Nicolet, C. Piras, P. Legrand, C.E. Hatchikian, J.C. Fontecilla-Camps, *Structure* 7 (1999) 13–23.
- Y. Nicolet, A.L. De Lacey, X. Vernède, V.M. Fernandez, E.C. Hatchikian, J.C. Fontecilla-Camps, *J. Am. Chem. Soc.* 123 (2001) 1596–1601.
- A.J. Pierik, M. Hulstein, W.R. Hagen, S.P.J. Albracht, *Eur. J. Biochem.* 258 (1998) 572–578.
- A.L. De Lacey, C. Stadler, C. Cavazza, E.C. Hatchikian, V.M. Fernandez, *J. Am. Chem. Soc.* 122 (2000) 11232–11233.
- Z. Chen, B.J. Lemon, S. Huang, D.J. Swartz, J.W. Peters, K.A. Bagley, *Biochemistry* 41 (2002) 2036–2043.
- F. Gloaguen, J.D. Lawrence, M. Schmidt, S.R. Wilson, T.B. Rauchfuss, *J. Am. Chem. Soc.* 123 (2001) 12518–12527.
- E.J. Lyon, I.P. Georgakaki, J.H. Reibenspies, M.Y. Darensbourg, *J. Am. Chem. Soc.* 123 (2001) 3268–3278.
- M. Razavet, S.C. Davies, D.L. Hughes, J.E. Barclay, D.J. Evans, S.A. Fairhurst, X. Liu, C.J. Pickett, *Dalton Trans.* (2003) 586–595.
- L.-C. Song, J. Cheng, J. Yan, H.-T. Wang, X.-F. Liu, Q.-M. Hu, *Organometallics* 25 (2006) 1544–1547.
- J.-F. Capon, S.E. Hassnaoui, F. Gloaguen, P. Schollhammer, J. Talarmin, *Organometallics* 24 (2005) 2020–2022.
- F.I. Adam, G. Hogarth, I. Richards, B.E. Sanchez, *Dalton Trans.* (2007) 2495–2498.
- J.D. Lawrence, H. Li, T.B. Rauchfuss, *Chem. Commun.* (2001) 1482–1483.
- L.-C. Song, J.-H. Ge, X.-G. Zhang, Y. Liu, Q.-M. Hu, *Eur. J. Inorg. Chem.* (2006) 3204–3210.
- J.-F. Capon, F. Gloaguen, P. Schollhammer, J. Talarmin, *Coord. Chem. Rev.* 249 (2005) 1664–1676.
- L.-C. Song, Z.-Y. Yang, H.-Z. Bian, Y. Liu, H.-T. Wang, X.-F. Liu, Q.-M. Hu, *Organometallics* 24 (2005) 6126–6135.
- L.-C. Song, Z.-Y. Yang, Y.-J. Hua, H.-T. Wang, Y. Liu, Q.-M. Hu, *Organometallics* 26 (2007) 2106–2110.
- A.Q. Daraosheh, M.K. Harb, J. Windhager, H. Görls, M. El-Khateeb, W. Weigand, *Organometallics* 28 (2009) 6275–6280.
- M.K. Harb, U.-P. Apfel, T. Sakamoto, M. El-khateeb, W. Weigand, *Eur. J. Inorg. Chem.* (2011) 986–993.
- (a) D.M. Heinekey, *J. Organomet. Chem.* 694 (2009) 2671–2680; (b) C. Tard, C.J. Pickett, *Chem. Rev.* 109 (2009) 2245–2274.
- L.-C. Song, M.-Y. Tang, F.-H. Su, Q.-M. Hu, *Angew. Chem. Int. Ed.* 45 (2006) 1130–1133.
- L.-C. Song, M.-Y. Tang, S.-Z. Mei, J.-H. Huang, Q.-M. Hu, *Organometallics* 26 (2007) 1575–1577.
- L.-C. Song, L.-X. Wang, M.-Y. Tang, C.-G. Li, H.-B. Song, Q.-M. Hu, *Organometallics* 28 (2009) 3834–3841.
- A.M. Kluwer, R. Kapre, F. Hartl, M. Lutz, A.L. Spek, A.M. Brouwer, P.W.N.M. van Leeuwen, J.N.H. Reek, *PNAS* 106 (2009) 10460–10465.
- A.P.S. Samuel, D.T. Co, C.L. Stern, M.R. Wasielewski, *J. Am. Chem. Soc.* 132 (2010) 8813–8815.
- E.J. Kuhlmann, J.J. Alexander, *Inorg. Chim. Acta* 34 (1979) 197–209.
- D.W. Thomas, A.E. Martell, *J. Am. Chem. Soc.* 81 (1959) 5111–5119.
- B.C. Bookser, T.C. Bruice, *J. Am. Chem. Soc.* 113 (1991) 4208–4218.
- L.-C. Song, B.-S. Yin, Y.-L. Li, L.-Q. Zhao, J.-H. Ge, Z.-Y. Yang, Q.-M. Hu, *Organometallics* 26 (2007) 4921–4929.
- E.J. Lyon, I.P. Georgakaki, J.H. Reibenspies, M.Y. Darensbourg, *Angew. Chem. Int. Ed.* 38 (1999) 3178–3180.
- L.-C. Song, C.-G. Li, J. Gao, B.-S. Yin, X. Lio, X.G. Zhang, H.-L. Bao, Q.-M. Hu, *Inorg. Chem.* 47 (2008) 4545–4553.
- (a) S.J. Silvers, A. Tulinsky, *J. Am. Chem. Soc.* 89 (1967) 3331–3337; (b) J.L. Sessler, M.R. Johnson, S.E. Creager, J.C. Fetting, J.A. Ibers, *J. Am. Chem. Soc.* 112 (1990) 9310–9329.
- D. Seyferth, R.S. Henderson, L.-C. Song, *J. Organomet. Chem.* 192 (1980) C1–C5.
- J.L. Stanley, T.B. Rauchfuss, S.R. Wilson, *Organometallics* 26 (2007) 1907–1911.
- M. Razavet, S.C. Davies, D.L. Hughes, C.J. Pickett, *Chem. Commun.* (2001) 847–848.
- L.-C. Song, J. Yan, Y.-L. Li, D.-F. Wang, Q.-M. Hu, *Inorg. Chem.* 48 (2009) 11376–11381.
- (a) N.G. De Kimpfe, M.T. Rocchetti, *J. Agric. Food Chem.* 46 (1998) 2278–2281; (b) T. Anada, R. Karinaga, M. Mizu, K. Koumoto, T. Matsumoto, M. Numata, S. Shinkai, K. Sakurai, e-J. Surf. Sci. Nanotechnol. 3 (2005) 195–202.
- D. Seyferth, R.S. Henderson, L.-C. Song, *Organometallics* 1 (1982) 125–133.
- CRYSTALCLEAR 1.3.6, Rigaku and Rigaku/MS, 9009 New Trail Dr. The Woodlands TX 77381 USA, 2005.
- G.M. Sheldrick, SHELXS97, a Program for Crystal Structure Solution, University of Göttingen, Germany, 1997.
- G.M. Sheldrick, SHELXL97, a Program for Crystal Structure Refinement, University of Göttingen, Germany, 1997.
- M.J. Frisch, G.W. Trucks, H.B. Schlegel, G.E. Scuseria, M.A. Robb, J.R. Cheeseman, G. Scalmani, V. Barone, B. Mennucci, G.A. Petersson, H. Nakatsuji, M. Caricato, X. Li, H.P. Hratchian, A.F. Izmaylov, J. Bloino, G. Zheng, J.L. Sonnenberg, M. Hada, M. Ehara, K. Toyota, R. Fukuda, J. Hasegawa, M. Ishida, T. Nakajima, Y. Honda, O. Kitao, H. Nakai, T. Vreven, J.A. Montgomery Jr., J.E. Peralta, F. Ogliaro, M. Bearpark, J.J. Heyd, E. Brothers, K.N. Kudin, V.N. Staroverov, R. Kobayashi, J. Normand, K. Raghavachari, A. Rendell, J.C. Burant, S.S. Iyengar, J. Tomasi, M. Cossi, N. Rega, J.M. Millam, M. Klene, J.E. Knox, J.B. Cross, V. Bakken, C. Adamo, J. Jaramillo, R. Gomperts, R.E. Stratmann, O. Yazyev, A.J. Austin, R. Cammi, C. Pomelli, J.W. Ochterski, R.L. Martin, K. Morokuma, V.G. Zakrzewski, G.A. Voth, P. Salvador, J.J. Dannenberg, S. Dapprich, A.D. Daniels, Ö. Farkas, J.B. Foresman, J.V. Ortiz, J. Cioslowski, D.J. Fox, Gaussian 09, Gaussian, Inc., Wallingford CT, 2009.